

## Performance Analysis of Magnetic Torquer for Spacecraft Control

Seon-Ho Lee\*, Hyun-Ho Seo\*\*, and Seung-Wu Rhee\*\*\*

\* Department of Satellite Control, Korea Aerospace Research Institute, Taejon, Korea  
(Tel : +82-42-860-2035; E-mail: shlee71@kari.re.kr)

\*\* Dept of Satellite Systems & Applications, University of Science and Technology, Taejon, Korea  
(Tel : +82-42-860-2557; E-mail: seo2h@ust.ac.kr)

\*\*\* Department of Satellite Control, Korea Aerospace Research Institute, Taejon, Korea  
(Tel : +82-42-860-2447; E-mail: srhee@kari.re.kr)

**Abstract:** This paper presents the overall design, manufacture, and test result of the high capacity (more than 150 Am<sup>2</sup>) magnetic torquer for the use of satellite control. To provide an electrical current to the magnetic torquer, the driving electronics is also constructed. The integration and test of the magnetic torquer and its driving electronics are performed via the magnetic field measurement according to the distance and the magnetic torque measurement with torque-meter. To compare the performance obtained from the test results we also perform computer simulation with three-dimensional model.

**Keywords:** Magnetic Torquer, Magnetic Field, Magnetic Dipole Moment, Driving Electronics

### 1. INTRODUCTION

The magnetic torquer (or torque rod) is a magnetic dipole moment generating device which produces torque with an interaction of geomagnetic field in space. The magnetic torquer is used in spacecrafts for attitude control instead of reaction wheels and thrusters, momentum dumping of reaction wheels, and compensation of magnetic residual inside the spacecraft in order to achieve a stable camera pointing capability during the mission [1-2]. Although the magnetic torquer produces smaller torque level than the reaction wheel and the thruster, it is mounted on the most satellites as a basic actuator owing to its simple structure and high reliability. In this paper, we present the details of design, manufacture, and initial test result of the high capacity magnetic torquer for the use of small satellites. Currently, three magnetic torquers whose momentum is expected to be more than 150 Am<sup>2</sup>, have been manufactured as a laboratory model and they are under various test. To provide a current to the magnetic torquer, the driving electronics is constructed. Furthermore, the computer simulation and experimental results are provided to compare with the requirements. This paper consists of the design and manufacture of the magnetic torquer and the driving electronics in Section 2, the computer simulation analysis in Section 3, the experimental results in Section 4, and the Conclusions in Section 5.

### 2. DESIGN & MANUFACTURE

#### 2.1 Magnetic Torquer (MTQ)

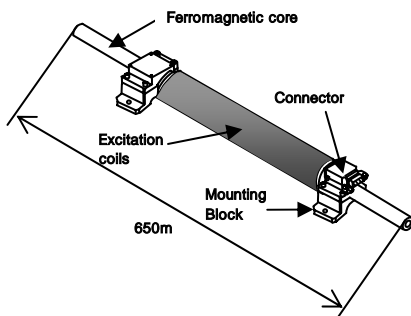


Figure 1 Structure of magnetic torquer

The magnetic torquer is an electromagnet which is composed of ferromagnetic cylindrical core wound with the excitation coil as shown in figure 1. The excitation coil current ( $I$ ) induces the magnetic field ( $B$ ) and the volume integral of the magnetic field generates the magnetic dipole moment ( $M$ ). Thus, as shown in figure 2 the dipole moment produces the torque ( $T$ ) which rotates the spacecraft in space by interacting with the geomagnetic field ( $B_E$ ) such as  $T = M \times B_E$ .

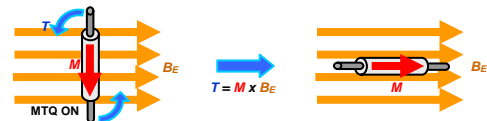


Figure 2 Interaction of MTQ with geomagnetic field ( $B_E$ )

In most cases, the current coil of the magnetic torquer is wound dually for primary and redundant usage to cover the single failure situation. In electrical point of view, the magnetic torquer is modeled as a serial connection of resistor, inductor, and residual capacitor between the coils. Moreover, the magnetic torquer is mathematically modeled with a single current loop approximately. In figure 3, the measurement position angle from the axial axis at center of the loop is denoted by  $\theta$ , the distance of measurement position from the center by  $R$ , and the total measured magnetic field at given position by  $B$ . Here, we note that  $B_R$  and  $B_\theta$  are the radial and tangential components such as

$$B(R, \theta) = B_R \vec{R} + B_\theta \vec{\theta} = \frac{\mu_0 M}{4\pi |R|^3} (2 \cos \theta \vec{R} + \sin \theta \vec{\theta}) \quad (1)$$

Moreover, the dipole moment is computed as

$$M = \frac{1}{\mu_0} \int_V B dV = B(R, 0) \frac{2\pi R^3}{\mu_0} \quad (2)$$

The above equation is an approximated results by assuming that  $R$  is sufficiently larger than the current loop radius where  $\mu_0$  ( $=4\pi \times 10^{-7}$  H/m) is the vacuum permeability. Particularly, for the cases of  $\theta=0$  and  $\pi/2$ , we obtain

$$B(R, 0) = \frac{\mu_0 M}{2\pi |R|^3} \vec{R}$$

$$B(R, \frac{\pi}{2}) = \frac{\mu_0 M}{4\pi |R|^3} \vec{\theta}$$
(3)

According to the above equations, the dipole moment can be calculated from the measured magnetic field distribution and the generated torque is estimated.

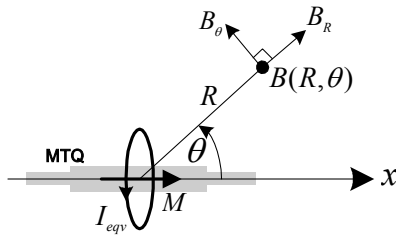


Figure 3 Magnetic field of single current loop

The requirement specification of the designed magnetic torquer with high dipole moment capacity is described as follows:

- Coil resistance: 78 Ohm
- Coil inductance: 13 H
- Generated magnetic dipole moment: > 150 Am<sup>2</sup>
- Max applied voltage: +/- 15V
- Coil turn number: 6546
- Coil length: 33.8
- Core: Ni-Alloy with high permeability
- Core dimension (D x L): 22mm x 650mm
- Total mass: 5 kg
- Max power: < 3 W

As shown in figure 2, the manufactured magnetic torquer is equipped with two mounting blocks for spacecraft installation and a D-type connector for the driving current interface with on-board computer.



Figure 4 Photo of magnetic torquer

### 2.2 Driving Electronics (TDE)

The driving electronics is designed to provide the coil current to the magnetic torquer according to the control command. It reads the 12-bit digital command from the on-board computer of the satellite and outputs a corresponding analog voltage in the range of -15V~+15V to the magnetic torquer.

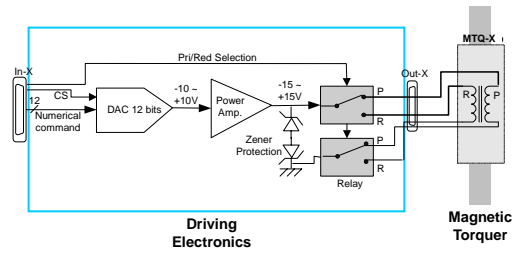


Figure 5 Circuit of driving electronics

Inside the driving electronics, the electrical circuit board is composed of 12-bit digital-to-analog converter, power amplifier, and the two relay making it easy to select the primary and redundant coils of the magnetic torquer as shown in figure 5. Owing to the driving electronics, bang-bang and/or proportional control action according to the specific control algorithm can be implemented. Outside the box, three LED lamps are installed to indicate the on/off status of the primary and redundant coil excitation in the front panel and three input/output connectors (X,Y,Z) are installed in the back panel.



Figure 6 Photo of driving electronics

### 3. Computer Simulation

In this paper, we execute the computer simulation for the performance analysis of the magnetic torquer. As shown in figure 7, the three-dimensional model of the magnetic torquer is performed with the following steps: (i) define structure of magnetic torquer, (ii) set boundary conditions, (iii) define current sources, (iv) solve the magnetic field density, (v) compute the magnetic dipole moment by post-processing. Figure 8-9 show the estimated magnetic field  $B_x(X=0,Y,Z)$  at Y-Z plane and  $B_x(X,Y=0,Z)$  at X-Z plane. The simulation results reveal that the magnetic field are induced dominantly inside the core and the maximum field magnitude along the axial direction is about 1.1Tesla (=11,000 Gauss). We note that the geomagnetic field normally amounts to -0.6~+0.6 Gauss on ground.

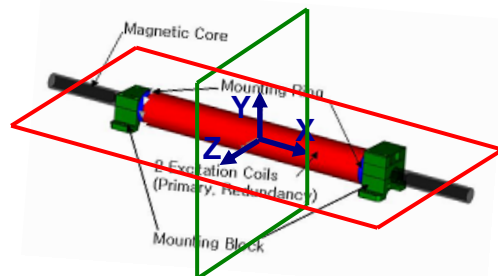


Figure 7 Three-dimensional model of magnetic torquer

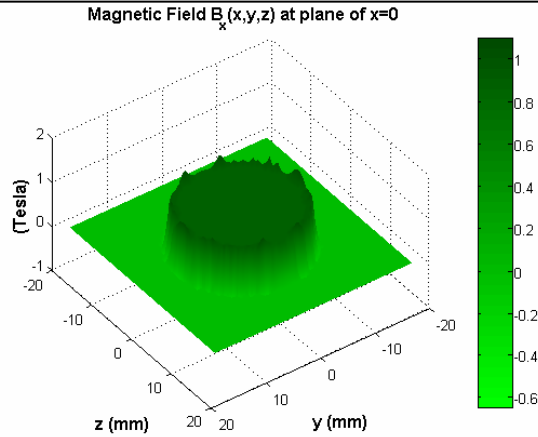


Figure 8 Magnetic field  $B_x$  at X-Z plane (when  $Y=0$ )

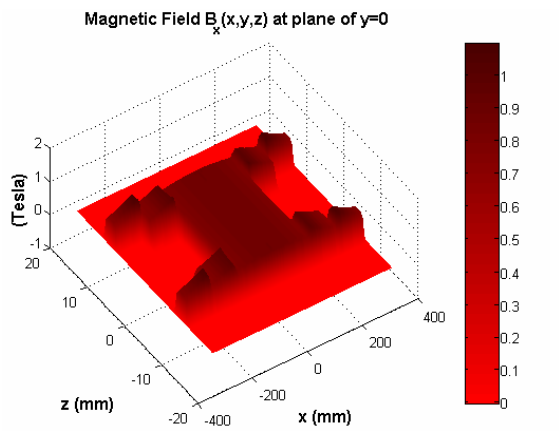


Figure 9 Magnetic field  $B_x$  at Y-Z plane (when  $X=0$ )

Using the simulation data, we calculate the magnetic dipole moment by volume integration of the magnetic field distribution as follows.

$$\begin{aligned}
 M &= \frac{1}{\mu_0} \int_V B dV \\
 &= \frac{2\pi}{\mu_0} \iint B(r, z) r dr dz \\
 &= 180 \text{ Am}^2
 \end{aligned}
 \tag{4}$$

According to the above calculation, we can check the estimated dipole moment satisfies the minimum requirement of  $150 \text{ Am}^2$ .

#### 4. Experiment

##### 4.1 Magnetic Field Measurement

One of the well known methods to check the dipole moment is to measure the magnetic field magnitude depending on the measurement distance from the excited magnetic torquer. This method is very simple but it needs magnetically calm environment by minimizing the external magnetic disturbance source and noise coming from the magnetic materials.

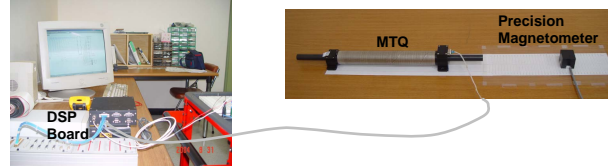


Figure 10 Photo of magnetic field measurement test setup

The test setup consists of magnetic torquer, driving electronics, DSP board, control PC, and precision magnetometer. The test is done by measuring the magnetic field magnitude along the axial direction of the magnetic torquer. Recall that

$$B_x = \frac{\mu_0 M}{2\pi |x|^3} = \frac{a}{|x|^3}, \quad (a \triangleq \frac{\mu_0 M}{2\pi})
 \tag{5}$$

where  $a$  is a scale factor to be determined. By gathering the measured magnetic field data and its corresponding distance and applying to the above equation, we can plot figure 11. By 1<sup>st</sup> order curve fitting of the measurement data, we obtain

$$a = 3.7 \times 10^{-5}
 \tag{6}$$

$$M = a \times \frac{2\pi}{\mu_0} = 186 \text{ Am}^2$$

The obtained dipole moment from the test results in (6) is quite similar with the estimated one from the computer simulation in (4).

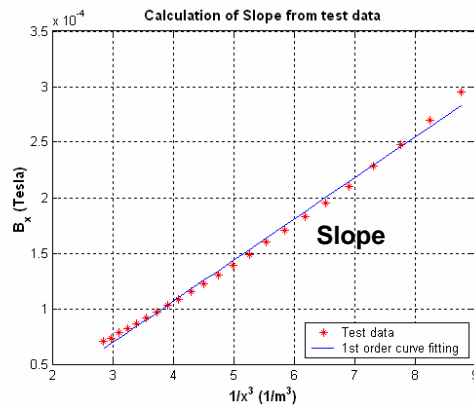


Figure 11 Calculation of slope ( $a$ ) with measurement data

##### 4.2 Magnetic Torque Measurement

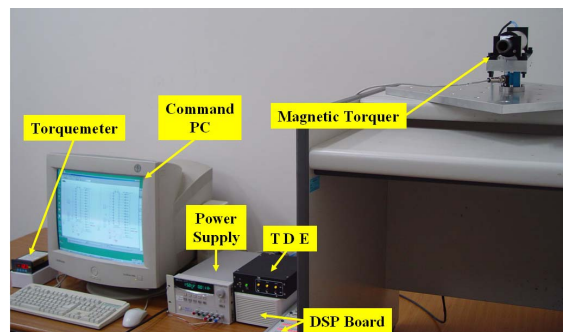


Figure 12 Photo of magnetic torque measurement test setup

We make an experiment on the magnetic torquer with a torque-meter. To compute its dipole moment, the geomagnetic field should be measured through the precision magnetometer, which has a different coordinate from the magnetic torquer. The magnetic torquer and the torque-meter are instrumented

on the table as shown at figure 12. The following formula represents the computing procedure of dipole moment and the coordinate transformations.

$$\vec{T} = \vec{M} \times \vec{B}_E$$

$$\begin{bmatrix} T_x \\ T_y \\ T_z \end{bmatrix} = \begin{bmatrix} \cos \theta & -\sin \theta & 0 \\ \sin \theta & \cos \theta & 0 \\ 0 & 0 & 1 \end{bmatrix} \begin{bmatrix} M_x \\ M_y \\ M_z \end{bmatrix} \times \begin{bmatrix} \cos 90^\circ & \sin 90^\circ & 0 \\ -\sin 90^\circ & \cos 90^\circ & 0 \\ 0 & 0 & 1 \end{bmatrix} \begin{bmatrix} \cos 180^\circ & 0 & -\sin 180^\circ \\ 0 & 1 & 0 \\ \sin 180^\circ & 0 & \cos 180^\circ \end{bmatrix} \begin{bmatrix} B_{x'} \\ B_{y'} \\ B_{z'} \end{bmatrix} \quad (7)$$

where

- $\vec{T}$  : Measured torque from torque-meter
- $\vec{M}$  : Dipole moment
- $\vec{B}_E$  : Geomagnetic field
- $\theta$  : Rotation angle from the reference frame
- $X - Y - Z$  : Fixed reference coordinate
- $x' - y' - z'$  : Magnetometer coordinate

Assuming that  $M_y \cong M_z \cong 0$ , the dipole moment is simply obtained as

$$T_z = M_x (B_{x'} \cos^2 \theta + B_{y'} \sin \theta \cos \theta + B_{z'} \sin^2 \theta - B_{y'} \sin \theta \cos \theta) \quad (8)$$

$$M_x = \frac{T_z}{B_{x'}} \quad (9)$$

The geomagnetic field is measured on three positions (left, center, and right) by putting the magnetometer on the plate in figure 13. The torque-meter measures the generated magnetic torque about the Z-direction. The command voltage to the magnetic torquer varies from +15V to -15V and its sequence is plotted in figure 14. As shown in Table 1, to minimize the measurement error of the test results, the magnetic torque and geomagnetic field data are gathered at different rotation angle of the plate such as  $\theta = 0^\circ, 45^\circ, 135^\circ$ .

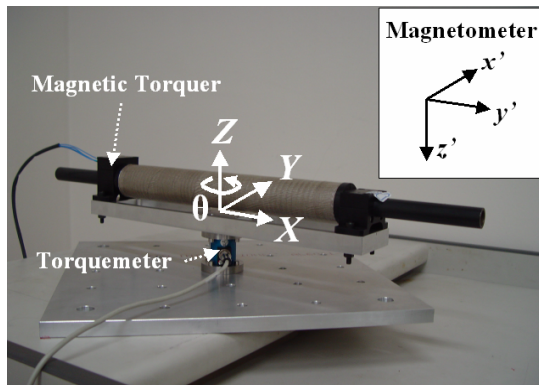


Figure 13 Coordinate definition

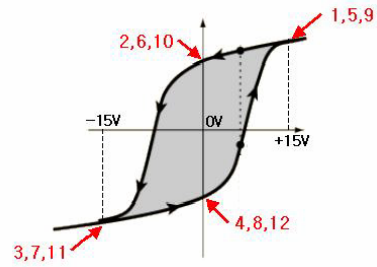


Figure 14 Command voltage cycling to magnetic torquer

Table 1 Measured magnetic torque from torque-meter

Voltage (V)	No.	Torque (mNm)		
		Rotation Angle $\theta$ (deg)		
		0	45	135
+15	1	2.1	1.3	-1.2
+0	2	0.0	0.0	0.0
-15	3	-2.9	-2.1	2.0
-0	4	-0.9	-0.7	0.7
+15	5	2.0	1.3	-1.2
+0	6	0.0	0.0	0.0
-15	7	-2.9	-2.1	1.9
-0	8	-0.9	-0.7	0.6
+15	9	2.1	1.4	-1.3
+0	10	0.0	0.0	0.0
-15	11	-2.9	-2.0	1.9
-0	12	-0.9	-0.6	0.6

Table 2 Measured field data from precision magnetometer

Rotation Angle (deg)	Geomagnetic Field ( $B_{x'}$ )			
	Left	Center	Right	Average
0	-23765	-22277	-22243	-22762
45	-15550	-16888	-17859	-16766
90	89.9	-1959	-2605	-1491
135	16583	13419	14044	14682

Figure 15 shows the calculated dipole moment by post-processing of the gathered data according to the command voltage cycling. The result reveals that the maximum magnetic torque is about 105 Am<sup>2</sup> on average and it seems to have a residual dipole moment of approximately 20Am<sup>2</sup>. This result which is different from (4) and (6), results from the performance limitation of the torque-meter. To investigate it more clearly, it should be noted that the measurement accuracy of the torque-meter is less about 1mNm. Thus, the torque-meter can't measure the generated torque ranging from -2mNm to 2mNm exactly, and the torque level corresponding to the residual dipole moment is too small for the torque-meter to measure the magnetic torque. Moreover, at the moment now it is too rush to conclude that 20Am<sup>2</sup> is the residual dipole moment and it comes from the inherent hysteresis characteristics of the magnetic core. Thus, it is believe that the magnetic torque measurement test results obtained by the limited torque sensing equipment gives not the quantitative but the qualitative performance of the magnetic torquer. To exact measurement of the generated torque level, more accurate

torque-meter should be engaged in the magnetically uniform environment without any noise source.

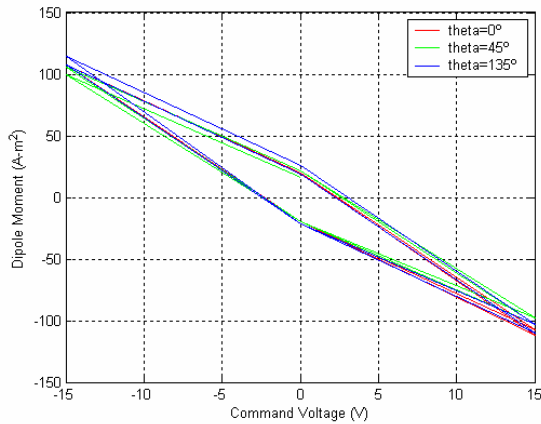


Figure 15 Dipole moment versus command voltage cycling

### 5. CONCLUSIONS

This paper presents the development of the magnetic torquer which is used in spacecrafts for the attitude control and momentum dumping. The magnetic torquer and its driving electronics is designed and tested via magnetic field measurement according to the distance and magnetic torque measurement with torque-meter. Furthermore, this paper performs computer simulation with three-dimensional model to compare it with the real test performance. Throughout the analysis and test experience as introduced in this paper, we achieve the fully understanding of the nature of the magnetic torquer and set up its development process of the future flight models for spacecraft control.

### REFERENCES

- [1] J.R. Wertz, "Spacecraft Attitude Determination and Control", D. Reidel Publishing Company, Holland, 1978.
- [2] M.J. Sidi, "Spacecraft Dynamics and Control - A Practical Engineering Approach", Cambridge University Press, 1997.
- [3] D.K. Cheng, Field and Wave Electro-magnetics, Addison-Wesley Pub., 1989.
- [4] J. Lee, A. Ng, R. Jobanputra, "On Determining Dipole Moments of a Magnetic Torquer Rod - Experiments and Discussion", J. Aeronautique et Spatial De Canada, vol. 48, no. 1, pp. 61-67, 2002.
- [5] B.V. Rauschenbakh, M.Y. Ovchinnikov, and S. Mckenna-Lawlor, Essential Spaceflight Dynamics and Magnetospherics, Kluwer Academic Publishers
- [6] P. Nakmahachalasint, K.D.T. Ngo, and L. Vu-Quoc, "Effective Magnetic Parameters in the Presence of Hysteresis", IEEE Trans Aerospace & Electronic Systems, Vol. 40, No. 3, pp 1100-1104, 2004.